Polarizability effects on the structure and dynamics of ionic liquids

Ary de Oliveira Cavalcante' , Mauro C. C. Ribeiro, and Munir S. Skaf

Citation: The Journal of Chemical Physics **140**, 144108 (2014); doi: 10.1063/1.4869143
View online: http://dx.doi.org/10.1063/1.4869143
View Table of Contents: http://aip.scitation.org/toc/jcp/140/14
Published by the American Institute of Physics

Polarizability effects on the structure and dynamics of ionic liquids

Ary de Oliveira Cavalcante,[1,2,a)] Mauro C. C. Ribeiro,[3] and Munir S. Skaf[1]
[1]*Institute of Chemistry, University of Campinas – UNICAMP, Cx. P. 6154, Campinas, SP 13084-862, Brazil*
[2]*Departamento de Química, Universidade Federal do Amazonas, Av. Rodrigo Octávio, 6200, Coroado, Manaus, AM, Brazil*
[3]*Laboratório de Espectroscopia Molecular, Instituto de Química, Universidade de São Paulo, São Paulo, SP C.P. 26077, 05513 970 São Paulo, SP, Brazil*

(Received 17 July 2013; accepted 10 March 2014; published online 11 April 2014)

Polarization effects on the structure and dynamics of ionic liquids are investigated using molecular dynamics simulations. Four different ionic liquids were simulated, formed by the anions Cl^- and PF_6^-, treated as single fixed charge sites, and the 1-*n*-alkyl-3-methylimidazolium cations (1-ethyl and 1-butyl-), which are polarizable. The partial charge fluctuation of the cations is provided by the electronegativity equalization model (EEM) and a complete parameter set for the cations electronegativity (χ) and hardness (J) is presented. Results obtained from a non-polarizable model for the cations are also reported for comparison. Relative to the fixed charged model, the equilibrium structure of the first solvation shell around the imidazolium cations shows that inclusion of EEM polarization forces brings cations closer to each other and that anions are preferentially distributed above and below the plane of the imidazolium ring. The polarizable model yields faster translational and reorientational dynamics than the fixed charges model in the rotational-diffusion regime. In this sense, the polarizable model dynamics is in better agreement with the experimental data. © *2014 AIP Publishing LLC*. [http://dx.doi.org/10.1063/1.4869143]

I. INTRODUCTION

The typical inorganic ionic compounds present high melting points and form crystalline solids at room temperature, with a well defined structural order that results from the delicate balance between the long range electrostatic forces and the spatial arrangement of the ionic packing.[1,2] The first examples of molten salts at room temperature that contradicts this generic behavior dates back over a century ago, with the salts ethylammonium nitrate (m.p. 13–14 °C)[3] and ethanolammonium nitrate (m.p. 52–55 °C).[4] In the last two decades, however, we have witnessed a remarkable increase in the discovery of organic salts that are liquids at room temperature, the ionic liquids (ILs).

The basic definition of the ILs was consolidated for systems formed exclusively by charged species with a melting point below 100°C.[5] Some ILs are found in the liquid state at very low temperatures, ca. −90 °C.[6] ILs usually result from a combination of at least one large organic cation, such as the quaternary ammonium ion,[7] which carry a delocalized π electron cloud around a ring, such as imidazolium, pyridinium, or pyrrolidium, and an organic, inorganic, or halogenated organic anion such as halides, PF_6^-, BF_4^-, and $CF_3SO_3^-$. The large organic cation ring is typically connected to one or more alkyl side chains whose length strongly influences the properties of the system, including density, melting point, and vapor pressure, which is remarkably low, electrical conductivity, long range structure, and viscosity, to name a few.

Typical ILs present very slow dynamics, low ionic conductivity, high viscosity, and prominent structural and dynamical heterogeneities when compared to ordinary molecular liquids.[8] A comprehensive understanding of the molecular basis underlying the physical chemical properties of ILs is far from reached and, therefore, is currently of keen interest. In this regard, molecular dynamics (MD) computer simulations have been profitably used to unravel the behavior of ILs from an atomistic or molecular perspective. Due to the existence of a great number of possible combinations of cations and anions, Camper *et al.*[9] forecast a fine-tuning process into the design of the ILs according to specific applications. However, in practice, this possibility is hindered by the lack of universal simple rules predicting many of the basic ILs properties. Computer simulations results describing details of the equilibrium structure in ILs[10–12] have stressed the relative positions of anions around the cations in the bulk liquid. In the particular case of the 1-*n*-alkyl-3-methylimidazolium ILs, the first neighbor configuration is strongly related to the anion's ability to hydrogen (H) bond to the acid H2 of the cation.[13] The small halide anions are strongly H-bonded to the imidazolium cations and usually result in salts that are typically solid at room temperature, whereas larger and poorer H-bond acceptor anions like BF_4^-, PF_6^-, and triflate are able to form ionic compounds with quite lower melting points.

Nevertheless, one should be careful in assigning H-bond ability or a particular ion size and shape as the only factors to determine the degree of fluidity or even the melting points of the ionic liquid. In this sense, the lack of proper consideration of many other complex factors like ionic packing, covalent interactions, and ionic screening, other than H-bond

a)Author to whom correspondence should be addressed. Electronic mail: arycavalcante@ufam.edu.br

alone, may lead in some cases to the exact opposite conclusion concerning the traditional influence of H-bonds in the melting points.[14] From the theoretical point of view, the most challenging question refers to the choice of an adequate charge model, capable of reproducing the physico-chemical properties of ILs.[15] Polarizable molecular dynamics simulations emerge in this context as a natural theoretical requirement to those who pursuit a more realistic description of the strong interparticle interactions in ionic systems.[16–19]

Available interaction site models based on fixed partial charges do not seem to yield an accurate description of ILs dynamics.[15,20] The typical drawback of fixed charge models is the slow diffusivity and reorientational dynamics, by far distant from the available experimental data.[21] There is compelling evidence that the lack of polarizability in these models is the main source of discrepancies between simulation and experimental data on self-diffusion coefficients.[22] The inclusion of more complex electronic phenomena like liquid charge transfer between the ionic species may also play a role in accelerating simulated dynamics.[23]

The aim of this work is to evaluate the impact of the cationic polarizability into the structure and dynamics of the archetypical ionic liquids. Here, we use the electronegativity equalization method (EEM) to obtain a new polarizable model for the imidazolium family of ILs cations. We particularly show that there are marked changes in the distribution of the anions around the cations upon inclusion of the polarizability and that these structural changes promote a much faster dynamics of the ionic species in comparison to the parent fixed charge model, but still slower than the experimental diffusivity. The vibrational density of states obtained from the Fourier transform of the velocity auto-correlation functions of the ions indicate that the spectral line-shape component due to the anionic species is markedly affected by the polarizability of the cations. The simulations also show that taking polarizability into account improves the line shape of the vibrational spectrum in comparison to the experimental Raman spectrum.

This paper is organized as follows. In Sec. II, we present a brief description of the computational details and models used in this paper. In Sec. III, the theoretical foundations of EEM applied to the cations are briefly described. In Sec. IV, we present the results and discussion about the parameter set optimized for the polarizable model derived for the imidazolium cations family. In Sec. V, we report the structure and dynamics obtained from the polarizable model and compare with the results obtained with the fixed charge model. Concluding remarks are presented in Sec. VI.

II. COMPUTATIONAL DETAILS

The force field used in our simulations includes the typical short-range Lennard-Jones and the long-range Coulomb interaction terms between atoms that are not covalently bonded, and an intramolecular or bonded term that includes bond stretching, r, angle bending, θ, and dihedral torsions, ψ:

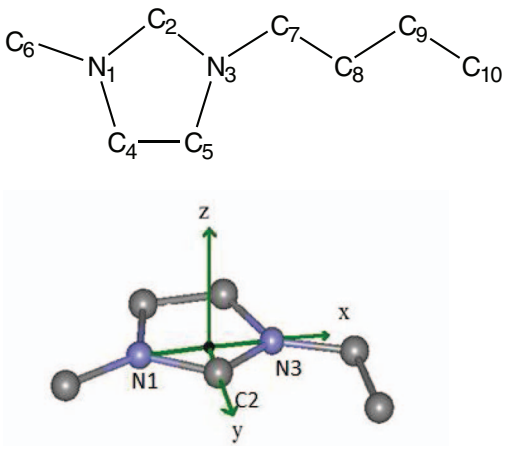

FIG. 1. Structure of the imidazolium cation as a united atom model and numbering scheme adopted in this work.

$$V(r_{ij}) = 4\varepsilon_{ij}\left[\left(\frac{\sigma_{ij}}{r_{ij}}\right)^{12} - \left(\frac{\sigma_{ij}}{r_{ij}}\right)^{6}\right] + \frac{q_i q_j}{4\pi\varepsilon_0 r_{ji}} + \sum_{bonds} k_b(r - r_{eq})^2 + \sum_{angles} k_\theta(\theta - \theta_{eq})^2 + \sum_{dihedrals} k_\psi\,[1 + \cos(n\psi - \delta)]^2, \quad (1)$$

where r_{ij} is the distance between the atoms i and j of different ions. The force field parameters are those previously proposed by Urahata and Ribeiro.[24] This model uses a united atom description for the hydrogen atoms of the cations as well as for the fluorine atoms in the hexafluorphosphate, PF_6^-, anions. Figure 1 shows a schematic representation of the chemical structure of the 1-alkyl-3-methylimidazolium cations with atom numbering. The ε and σ parameters were extracted from the optimized parameters for liquids simulation, OPLS.[25] Two different anions are considered in this work, Cl^- and PF_6^-, which are represented as single Lennard-Jones sites with a global charge of -1. The cations studied here were the following derivatives of the 3-methyl-imidazolium: 1-etil-3-methyl-imidazolium and 1-butyl-3-methylimidazolium, hereafter named $[emIm]^+$ and $[bmIm]^+$. The parameter set for the short range potential function includes the inter- and intramolecular potential terms. The intramolecular part contains the quadratic terms for the stretching, bending, and dihedral torsions. Four different ILs systems were simulated: [emIm]Cl, [bmIm]Cl, [emIm]PF_6, and [bmIm]PF_6. For comparison purposes, results obtained from simulations with the fixed charge models for the cations are also presented.

We used the cubic box containing 200 cations and 200 anions at equilibrium pressure of 1.0 bar, maintained by means of a Berendsen's barostat.[26] The temperature chosen for all the simulations was 400 K. The long-range electrostatic interactions were treated by means of the Ewald summation method. The Verlet algorithm was used for the integration of the equation of motions with a time step of 0.5 fs and 3.0 fs for the polarizable and fixed charge models, respectively. The

production runs lasted 3 ns for each system, performed in a NVE ensemble.

III. THEORETICAL BACKGROUND

The electronegativity equalization principle, formulated by Sanderson[27] in the 1950s, states that the partial atomic charges that results from the chemical bonding between two different atoms are those for which the atomic electronegativities are equal (Sanderson's electronegativity). The density functional theory[28] is the theoretical basis for the electronegativity equalization method, EEM, because the electronegativity equalization is a consequence of the minimization of the energy functional. The EEM allows for the fast calculation of the atomic charges in polyatomic systems by simple matrices equations without the direct application of the expensive Kohn-Sham methods.

The atomic site electronegativity depends on its charge and the electronegativity of the neighbor atoms. Parr and Pearson[29] showed that the Mulliken electronegativity of one atom is the negative of the chemical potential of the electron gas cloud around this atom,

$$\mu_{i\alpha} = \frac{\partial U}{\partial N_e} = -\chi_{i\alpha} = -e\frac{\partial U}{\partial q_{i\alpha}}, \tag{2}$$

where U is the electronic energy of the ground state, N_e is the number of electrons in the atom (treated as a continuous variable), q is the charge of the atom of the molecule i, and e is the elementary charge. In a polyatomic system, the electron gas will reach the equilibrium adiabatically in such a way that the chemical potential will be equal for all atomic sites. For this reason, the EEM is also known as the chemical potential equalization method. According to this view, the electron clouds will move from low electronegativity atoms (high chemical potential) to atoms with high electronegativity (low chemical potential).

The energy required to create a partial charge q at atom α of the molecule i can be expanded as the following series:

$$E(q_{i\alpha}) = E_{i\alpha}(0) + \chi^0_\alpha q_{i\alpha} + \frac{1}{2}J^0_{\alpha\alpha}q^2_{i\alpha}, \tag{3}$$

where χ and J are the empirical parameters known as electronegativity and hardness, respectively. These parameters depend on the atomic type and its chemical environment (number of chemical bonds, oxidation state, etc.).

The electrostatic energy of a system with N molecules, each molecule with n atoms, is given by the charge series expansion,

$$U(\{\mathbf{r}^N, \mathbf{q}^N\}) = \sum_{i=1}^{N_{molec}}\sum_{\alpha=1}^{N_{atom}}\left[E_\alpha(0) + \chi^0_\alpha q_\alpha + \frac{1}{2}J^0_{\alpha\alpha}q^2_\alpha\right] + \sum_{i\alpha<j\beta} J_{\alpha\beta}(r_{i\alpha j\beta})q_{i\alpha}q_{j\beta}. \tag{4}$$

Taking the derivative of Eq. (4) with respect to the charge of atom α of the molecule i, yields the instantaneous electronegativity,

$$\chi_{i\alpha} = \chi^0_\alpha + J^0_{\alpha\alpha}q_{i\alpha} + \sum_{\alpha\neq\beta} J_{\alpha\beta}(r_{i\alpha j\beta})q_{i\beta} + \sum_{j\neq i}\sum_{\beta} J_{\alpha\beta}(r_{i\alpha j\beta})q_{j\beta}. \tag{5}$$

In this version of the model, there is no intermolecular charge transfer and the sum of the partial charges is the global charge of the species, q,

$$\sum_{\alpha=1}^{N_{atom}} q_{i\alpha} = q. \tag{6}$$

The set of coupled linear equations involving the atomic charges is usually expressed in matrix form by

$$\mathbf{JQ} = \boldsymbol{\chi}, \tag{7}$$

where $\mathbf{Q}$ is a column matrix containing the charges for one chemical species.

It is worth to mention that the EEM is classified as a pure charge model and alternative approaches have been made in attempt to treat the polarization in molecular dynamics simulations. One alternative way to model the polarizability consists in connecting every atom of the polarizable species to a Drude oscillator. The Drude oscillator particles are characterized fundamentally by (i) its low weight compared to the atoms they are bounded to, (ii) to carry a small charge which subtracted from the charge of the bounded atom, and (iii) to its mobility as a function of the interactions. Another alternative to take into account the effects of electronic polarizability is to include many-body induced dipole interactions arising from site polarizability models incorporated into the force field.[16,17] Both approaches have their particular strengths and drawbacks in terms of computational costs and accuracy.[30] In turn, one of the drawbacks of our polarizable model is that it lacks the description of the out of ring plane polarizability, as well as at least one important interaction like anion to cation charge transfer that until now seems to be unveiled.

IV. CALIBRATION OF THE EEM PARAMETERS

The goal of calibrating is to achieve a parameter set that is able to produce EEM charges as close as possible to those calculated by standard quantum chemistry methods.[31–33] In this work, the parameters χ and J were adjusted such that the EEM charges could reproduce de Mulliken charges obtained by quantum chemical calculations at the MP2 level, with the basis function 6-311G*. The geometric conformations of the species for the ground state of the cations where performed at the same level using Gaussian.[34] A data bank of partial atomic charges for the cations in vacuum and probe charges in several different positions placed around the cations was then generated. The hydrogen charges were summed into the carbon atoms. Parameter set optimization was obtained using the SIMPLEX algorithm.[35] It is important to mention that we considered the chemical differences between the atoms, that is, for the smaller $[mmIm]^+$ cation, it was applied constrains in order to consider the structural symmetry for the $[emIm]^+$

TABLE I. Empirical EEM parameters for 1-alkyl-3-methyl-imidazolium cation that best reproduces the quantum chemical calculations with Mulliken charges.

	$[mmIm]^+$		$[emIm]^+$		$[bmIm]^+$	
	χ	J	χ	J	χ	J
N1	4.61	16.85	4.61	16.85	7.33	20.00
C2	0.31	18.37	2.00	13.72	3.31	18.65
N3	4.61	16.85	4.61	16.85	6.59	20.00
C4	3.42	12.59	3.02	13.14	3.00	20.00
C5	3.42	12.59	6.47	11.36	3.00	19.74
C6	0.18	23.69	1.07	20.47	4.74	23.17
C7	0.18	23.69	1.68	25.00	3.93	21.56
C8			2.35	25.00	4.73	19.61
C9					5.81	23.08
C10					7.18	23.16

and $[bmIm]^+$. All parameters were allowed to flow freely until the convergence due to the breakdown of the chemical symmetry caused by the alkyl chain.

The Table I displays the EEM parameters calibrated for the imidazolium cations $[mmIm]^+$, $[emIm]^+$, and $[bmIm]^+$ modeled as united atoms and Mulliken type charges. For the simplest $[mmIm]^+$ cations, the parameter set was constrained in order to make use of the mirror type symmetry. For the other cations, all EEM parameters were allowed to flow freely for each atom of the imidazolium cations, so that the different chemical environments around the atoms are taken into account. For comparison, Table II displays some EEM parameters proposed by other authors for the same atoms investigated. All parameters are within the typical range of the parameters available in the literature. A quantitative assessment of the reproducibility of the quantum chemical Mulliken charges by the EEM model is appreciated in Figure 2. The parameter optimization method is also capable of reproducing the magnitude of the total dipole moments, as shown in Figure 3. We observe a natural increase of the values of the dipole moment with increasing length of the alkyl chain of the imidazolium cation. This fact is reproduced by the present EEM procedure as well as by the Mulliken charges.

The optimization of the EEM parameters for a family of cations of similar structure allows asserting the chemical meaning based on the electronic structures of the cations. In general, the high chemical stability of the imidazolium cations is attributed to the delocalized π electrons cloud around the ring. This feature is captured by the EEM parameters since the J parameters of the chain are greater than those for the ring atoms.[36]

TABLE II. Some values for the EEM parameters (eV) collected on the literature.

	Bultnik *et al.*[a]		van Genechten *et al.*[b]	
	χ	J	χ	J
C	5.25	9.00	5.7	9.1
N	8.80	9.00	10.6	13.2

[a]Reference 31.
[b]Reference 55.

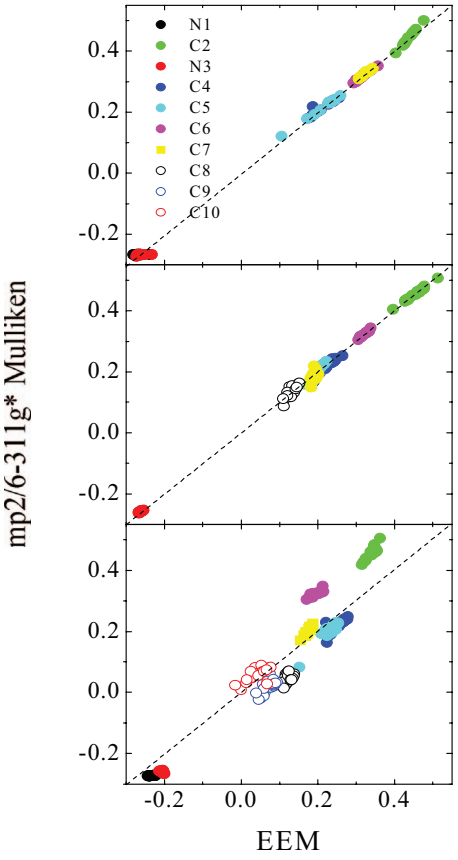

FIG. 2. Comparison of EEM and MP2 Mulliken point charges for all atoms of the cations $[mmIm]^+$ (top), $[emIm]^+$ (middle), and $[bmIm]^+$ (bottom) obtained using the parameters calibrated in this work and listed in Table I.

In the systems studied here, the aromatic imidazolium cations display the fundamental role on the overall properties of the imidazolium based ILs and, for the purposes of this work, the anions polarizability have been neglected under the expectation that the changes in the structural and dynamical properties of the systems are minor. In fact, molecular dynamics simulations performed on several ionic liquids containing

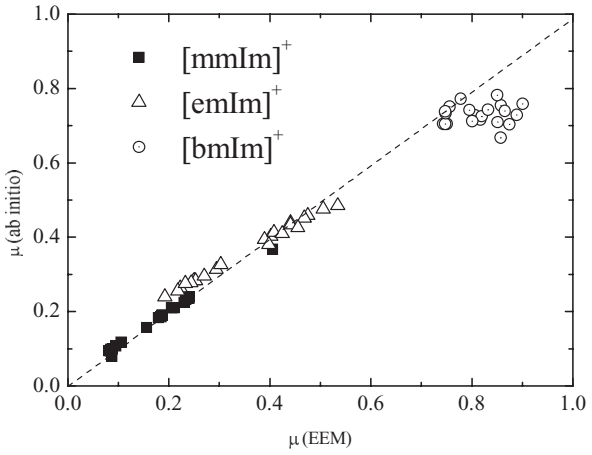

FIG. 3. Correlation diagram for the total dipole calculation from *ab initio* quantum chemical and EEM calculations. For each configuration, the cation is subjected to a field generated by a probe charge. The EEM charges were obtained using the parameters calibrated in this work and listed in Table I.

BF_4^- and PF_6^- anions, amongst others, have shown that inclusion of anionic polarizability have minor impacts on the structure, density, and dynamics of the ILs.[37] In addition, gas phase quantum chemistry calculations suggest that BF_4^- and PF_6^- have polarizabilities three times smaller than the imidazolium cations.[37]

V. SIMULATION RESULTS

A. Structure

From the cations atomic charge histograms depicted in the Figure 4, we note the degree of shift from the gas phase values, as well as the overall dispersion around an average value of the atomic point charges along the simulations of the [emIm]PF_6 and [bmIm]PF_6 systems. The atomic charge histograms give preliminary information about the environmental forces on the cations partial charge fluctuations. The overall changes are strongly felt by the cations in the [emIm]PF_6 salt, with large shifts from the gas phase values and strongly overlapped distributions. For the $[bmIm]^+$, the average values of the atomic charges in the liquid remain close to their respective values in gas phase.

The neutron scattering provides one of the most suitable experimental information to validate the theoretical data on equilibrium liquid structure. However, only a few examples of ILs were investigated in detail by this technique. According to reports on the neutron scattering of the ILs formed by $[mmim]^+$ with the Cl^- and PF_6^-,[38] the distribution profile of the anions around the cations is explained according to the different abilities of the anions to form hydrogen bonds with the cations. The poor hydrogen bond former PF_6^- is more likely to be found right above and below the plane of the imidazolium ring, while the Cl^- anion lies in the plane defined by the imidazolium ring and pointing to the direction towards the H2 atom, assigned as the most acid hydrogen available. This distribution trend of the Cl^- around the H2 atom of the $[mmIm]^+$ is well captured by *ab initio* MD simulations.[39]

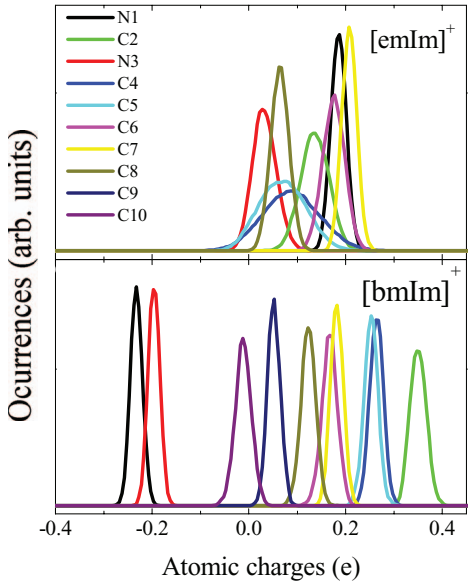

FIG. 4. Histograms of the imidazolium cations atomic charges calculated along the polarizable MD simulations of [emIm]PF_6 (top) and [bmIm]PF_6.

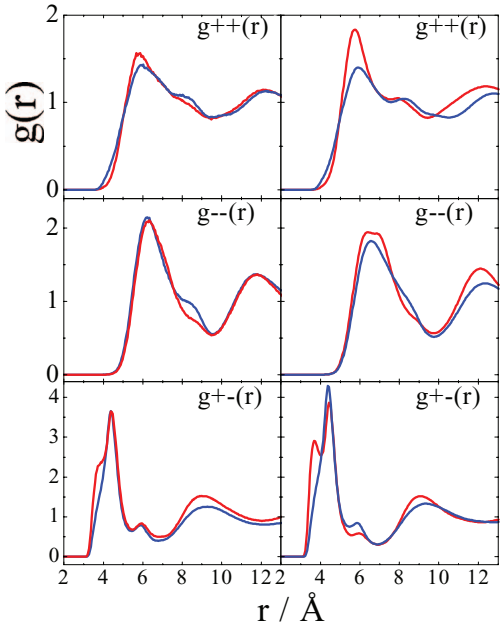

FIG. 5. Calculated radial distribution functions for the [emIm]Cl (left) and [bmIm]Cl at 400 K for the anions around the cation, anions around anions, and cations around cations for selected simulated systems. The geometric center of the imidazolium ring and the center of the anion were considered. Polarizable and fixed charge models are shown in red and blue lines, respectively.

The information about the changes on the relative distances with the inclusion of the cations polarizability emerges more readily from the partial radial distribution functions between cation–anion, $g_{\pm}(r)$, cation–cation, $g_{++}(r)$, and anion–anion, $g_{-}(r)$ shown in Figures 5 and 6 for ILs with Cl^- and PF_6^- anions, respectively. For comparison purposes, it is also

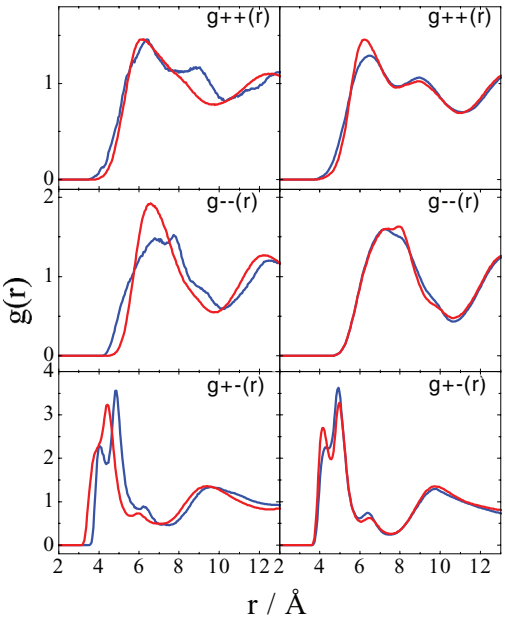

FIG. 6. Radial distribution functions between the geometric center of the imidazolium ring and the center of the anion for the [emIm]PF_6 (left) and [bmIm]PF_6 at 400 K for the anions around the cation, anions around anions, and cations around cations for selected simulated systems for the polarizable model (red lines) and fixed charge model (blue lines).

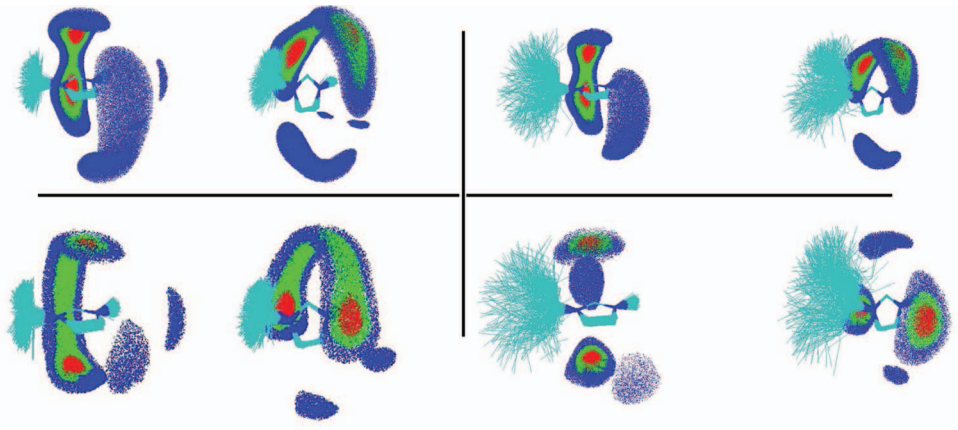

FIG. 7. Probability density maps of occurrence the first neighbor Cl^- anions around the imidazolium $[emIm]^+$ (left) and $[bmIm]^+$ (right) cations for the ionic liquids studied in this work in the charge fixed model (top) and polarizable model (botton). The top and bottom maps are for the charge fixed and polarizable models, respectively.

shown the equivalent data obtained with a charge fixed model (blue lines). The geometric center of the imidazolium ring was considered for the *g(r)* calculations.

The inclusion of the polarizability preserves the main structural characteristics of the ILs, as also observed by Yan *et al.*[16] The alternation of opposite charge ions is shown by the alternating positions of the peaks maxima and minima in $g_{++}(r)$ and $g_{-}(r)$. Due to the importance of the electrostatic interactions, the choice of the charge model strongly affects the nearest neighbor structure in IL.[40] As the anions of the first solvation shell around the imidazolium cations readily feel the cations charge, its structure is also sensitive to cations polarizability. Within the nearest neighbor range ($r < 6$ Å), $g_{\pm}(r)$ in the charge fixed model shows two superimposed peaks and the first one of them appears as a shoulder at shorter distances. The two overlapped peaks seen at short distances in $g_{\pm}(r)$ for [bmIm]Cl and $[bmIm]PF_6$ appear as two well separated peaks, with a smaller degree of overlap. This finding is in line with the neutron scattering experimental results for the liquid $[bmIm]PF_6$.[41] In general, the additional degree of freedom for the charges promotes a smoothing of the Coulombic forces when compared with the fixed charges model. These results suggest that polarization may allow a closer contact between the anions and cations in a sense that the repulsive Coulombic forces between particles of same charge types are dumped by the flow of charges in EEM. In this sense, there are clear structural changes on $[emIm]PF_6$, where $g_{\pm}(r)$ shows that the ions of different charges are closer to each other in the polarizable model. A similar effect was observed by Yan *et al.*[22] In the cases studied here, there is no apparent simple rule to predict which ion will be responsible for the greatest short range structural changes upon inclusion of the cation polarization. For instance, by simple inspection of the *g(r)* features, the structural changes promoted by the polarization of the light $[emIm]^+$ are larger when the counter ion is PF_6^-, but when the cation is the heavy $[bmIm]^+$, the small anion Cl^- forms the IL with greatest structural rearrangements upon polarization.

For a better understanding of the structural changes, it is useful to complement the information provided by *g(r)* with the shapes of the nearest neighbor probability density maps for anions around the imidazolium. Figures 7 and 8 show the probability density maps of Cl^- and PF_6^- anions, respectively, around $[emIm]^+$ and $[bmIm]^+$. Anions were selected whenever the distance to the geometric center of the imidazolium ring was smaller than the first minimum of the corresponding $g_{\pm}(r)$. Red, green, and blue areas in Figs. 6 and 8 indicate high (>80%), medium (60%–80%), and low

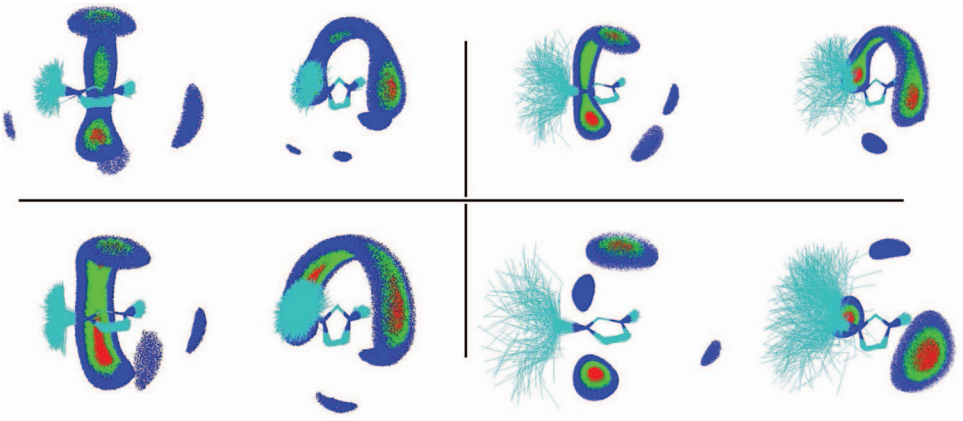

FIG. 8. Same as in Fig. 6 but for the PF_6^- anions.

(40%–60%) probabilities, respectively, of finding an anion around a given cation. Regions with probabilities lower than 40% of the maximum density of occurrences are not painted. For each system, the top panel shows the perspective from above the ring plane and the perspective on the plane of the ring for the charges fixed model, and the bottom panel for the polarizable model.

In the systems [emIm]Cl, [bmIm]Cl, and [bmIm]PF_6, we observe a clear and marked position shift of the volumes with high probability of finding anions, i.e., the red volumes, which are displaced from the vicinities of the C2 in the charge fixed model to places right above and below the center of the imidazolium ring in the polarizable model. We attribute this this phenomenon to a better distribution of the positive charge around the imidazolium ring in the polarizable model. In fact, it is known that the C2 is the most positive site of the imidazolium ring and it carries the most acid hydrogen assigned as the main hydrogen bond donor site.[42]

The basic average first neighbor H-bonded anions to the imidazolium cations in chloride based ILs appears to be an open topic. Despite the availability of detailed experimental information on the solid structure of the chlorine imidazolium salts,[43,44] there are still important experimental gaps in the literature concerning the structure of the molten chloride salts.[45] The high melting points of this systems, usually above 350 K[46] unables a clear technological application and even to the rough melting point limit used in the actual definition of ionic liquids. The influences of the charge model are then readily and strongly felt since the first shell around an ion may give rise to the plethora of possible first neighbors configurations, some of them discordant.[47,48] It is important to stress that the configuration presented here for the [emIm]Cl does not agree with the current prevailing view that there is a population of anions H-bonded to the H2 atom.

The kind of structure and the strength of the connection between the ions are of fundamental importance for the comprehension of the dynamical properties of the ILs. In a very simplistic view, a tightly bounded ionic pair by strong hydrogen bonds is one important feature that precludes the translational dynamics of the system. We also see that the green volumes around C2 also follow this trend in [bmIm]Cl and [bmIm]PF_6. The double peak shape in the $g_{\pm}(r)$ is then assigned to the splitting of the anions in two population distributions in the polarizable model: right above and below the center of the imidazolium ring and around the vicinities of the C2 atom.

B. Dynamics

The sluggish dynamics exhibited by ILs has been a subject of debate in the literature.[49,50] Several elements are included in the complex dynamics of the ions in IL. For instance, the long lived nearest neighbor shell comprised of opposite charge particles promotes the librational motions of the rings and the rattling motion of the particles, and hinders the translational diffusive dynamics of the ions. In addition, ILs have very low ionic conductivity as consequence of the reduced global charge displacements. The change in the dynamic properties of several kinds of liquids, molten salts, and ILs associated with the inclusion of polarizable models is discussed in several works (for a recent collection, see Ref. 51). In this case, there is an important connection between the structural changes discussed in Sec. V A and the changes of the dynamic rates of the process.

1. Residence times and reorientational dynamics

The time correlation function of the residence time, $C_{res}(t)$, is a useful means of obtaining a better understanding about the local dynamics around the imidazolium cations.[52] By definition, $C_{res}(t)$ is calculated using a Heaviside step function, $C_{res}(t) = \langle \theta_i(t) \cdot \theta_i(0) \rangle$, in which $\theta_i(t)$ is 1 when the anion i belongs to the first neighbor shell around the imidazolium cation and zero otherwise. The cut-off distance is set to the first minimum of the radial distribution function between the center of masses of the anions and cation rings, approximately 7 Å (see Fig. 1). The angle θ defined by the coordinates of the anions, the center of the imidazolium ring, and the z axis normal to the ring plane served as a criteria to split the total $C_{res}(t)$ into partial functions concerning only the anions inside the regions above and below the center of the imidazolium ring, $C_{res}^{top}(t)$, $\theta < 45^{\circ}$, and another function with anions surrounding the C2 atoms, $C_{res}^{HB}(t)$. The $C_{res}(t)$ function depicted in Figure 9 is highly nonexponential and suggests a complex dynamics of the anions around the imidazolium cations. The relaxation of $C_{res}^{top}(t)$ is much faster than $C_{res}^{HB}(t)$, indicating that the anions located in the anion crowded volume (red regions in Figs. 7 and 8) exhibit faster dynamics compared to the anions around the C2 site. Moreover, including polarizability effects into account leads to much faster decays of the ion pair residence time correlation function. For the ionic liquids formed by the Cl^-, the main change in the residence time correlation functions are clearly on the population that comprises the hydrogen bonded anions, $C_{res}^{HB}(t)$, which decays slightly faster in the

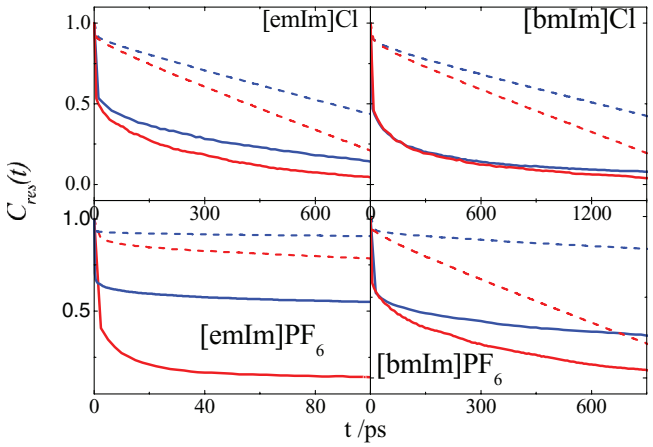

FIG. 9. Time correlation function of the residence time, partial *Cres(t)* for the anions above and below the imidazolium and around the C2 and the partial *Cres(t)* of the anions around the imidazolium cations in the fixed charges model (blue bold line and blue dashed line) and polarizable model (red bold lines and red dashed lines).

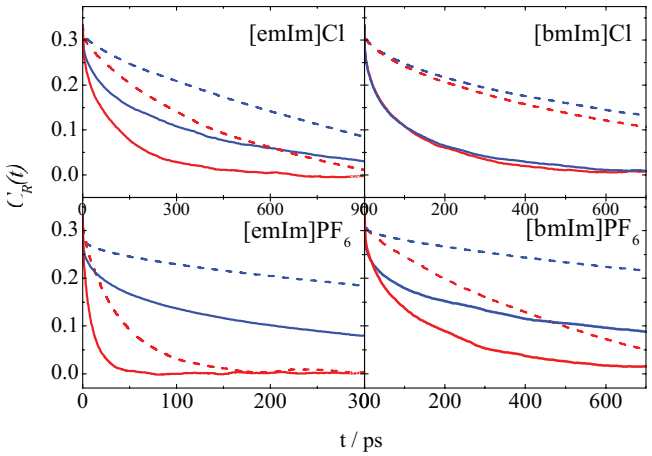

FIG. 10. Reorientational time correlation function of [emIm]Cl, [bmIm]Cl (top panels), [emIm]PF_6, and [bmIm]PF_6. For the $C_R(t)$ presented, we considered the dynamics of the NN direction (dashed lines) and the direction perpendicular to the imidazolium ring plane (bold lines) in the polarizable (red) and charge fixed (blue) models.

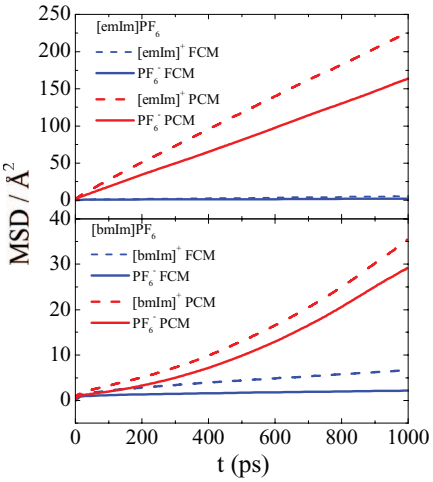

FIG. 11. Time dependence of the mean square displacements, MSD, of the cations (dashed lines) and anions (bold lines) in the polarizable (red lines) and charge fixed model (blue lines).

polarizable model. More prominent effects of polarizability forces are seen for the ionic liquids formed by the PF_6^-.

The reorientational dynamics was studied by the single particle time correlation function, $C_R(t) = \langle \mathbf{u_i}(t)\mathbf{u_i}(0)\rangle$, where $\mathbf{u}_i$ denotes a unit vector pointing along a conveniently chosen orthogonal directions (see Figure 1). Due to the geometrical anisotropy of the cations, three body-fixed directions were considered: along the main axis of the cations, i.e., along the direction defined by the atoms N1 and N3, along the center of mass-C2 direction, and perpendicular to the ring plane (directions x, y, and z, respectively, in Figure 1). The results are shown in Figure 10. As expected, $C_{Rx}(t)$ for the x direction shows the slowest component as it carries the alkyl chain which possesses the largest moment of inertia. $C_{Ry}(t)$ and $C_{Rz}(t)$ decay almost identically for any practical purposes. However, more important is that the reorientational dynamics is faster in all systems simulated with the polarizable model. For the [bmIm]Cl system, polarizability affects the reorientational dynamics only slightly. The relaxations of $C_R(t)$ and $C_{res}(t)$ follow similar trends in all systems studied. For example, we observe a faster decay of the $C_{res}^{HB}(t)$ in the polarizable model and very similar decay rates of $C_{res}^{top}(t)$ in both polarizable and fixed charge models (cf. Figure 8), while the reorientational dynamics shows a slightly faster decay for $C_{Rx}(t)$ with polarizability and similar decays for $C_{Ry}(t)$ and $C_{Rz}(t)$ for both models (Fig. 9). This shows that the anions hydrogen bonded to C2 are very important for the reorientational dynamics of the imidazolium cation.

2. Translational diffusion

The self-diffusion coefficient, D_i, for the ion i have been obtained from the long time regime of its mean square displacement (MSD), $\langle [r_i(t) - r_i(0)]^2\rangle$:

$$D_i = \lim_{t\to\infty} \frac{d}{dt}\frac{1}{6}\left\langle [r_i(t) - r_i(0)]^2 \right\rangle, \qquad (11)$$

where $\langle \ldots \rangle$ denotes ensemble average. The slow dynamics of the ILs is reflected on the self-diffusion coefficients of the cations and anions, D^+ and D^-. It is widely recognized that achieving true linear regime in the MSD of ILs is not a simple task. Our simulations may not be sufficiently long to generate reliable estimates for the diffusion coefficients, but nevertheless some qualitative information can be extracted from the mean square displacements. The typical value measured by NMR for ions in ILs at room temperature is 10^{-11} m^2s^{-1}, whereas the MSD value for ordinary molecular liquids at room temperature is of the order of 10^{-9} m^2s^{-1}. The MSD data shown in Figure 11 indicate that the cations are more mobile than the anions, despite the larger masses of the former. The calculations also show that this trend is preserved upon inclusion of polarizability. Previous MD simulations have shown that fixed charge models miss the experimental ion self-diffusion coefficients of ILs by at least one order of magnitude. The failure of fixed charge models to reproduce ILs dynamics have been attributed to the poor modeling of the anion as a single Lennard-Jones interaction site with a full charge of −1. Simulations performed with fixed charge models yield much slower diffusive dynamics for the PF_6^- ILs than that of the Cl^- liquids salts, despite the higher melting point of the latter, which is suggestive of stronger ionic interactions in Cl^- ILs.

Inclusion of polarizability increases the mobility of the ions for all systems, except for [bmIm]Cl, which undergoes a mild decrease in D^+ and D^-, as shown in Table III. The most pronounced changes take place for [bmIm]PF_6, for which the ions' self-diffusion coefficients increase some 10–40 fold. For this particular system, the values of D^+ (D^-) change from 0.68 (0.16) in the fixed charges model to 8.57 (7.14) for the polarizable model, in better agreement with the experimental values 20.91 (17.86).[53]

3. Fast dynamics and spectra for [emIm]PF_6

Figure 12 shows the velocity auto-correlation function VACF, $C_v(t) = \langle \mathbf{v}_i(t)\cdot\mathbf{v}_i(0)\rangle/\langle \mathbf{v}_i(0)^2\rangle$, where $\mathbf{v}_i(t)$ is the

TABLE III. Cation and anion diffusion coefficients, D^i (in 10^{-11} $m^2.s^{-1}$), for the ionic liquids from the present polarizable and charge fixed simulations at 400 K, the simulated diffusion coefficients are calculated from the Einstein relation.

	D^+			D^-		
System	*cfix*	*cflu*	Expt.	*cfix*	*cflu*	Expt.
[emIm]Cl	1.83	3.46		1.08	2.15	
[bmIm]Cl	3.23	2.90		1.60	1.26	
[emIm]PF_6	1.43	2.16		0.60	1.12	
[bmIm]PF_6	0.68	8.57	20.91	0.16	7.14	17.86

velocity of the center of mass of the imidazolium ring i at time t for the [emIm]PF_6 system using the fixed and polarizable charge models. In both models, the oscillatory features of $C_v(t)$ are more prominent for the cations than for the anions. For the polarizable model, both cations and anions exhibit somewhat less backscattering than with fixed charges. This behavior is consistent with the proposed view that polarization softens the Coulombic interactions.

The vibrational density of states, $DoS(\omega)$, is obtained from the Fourier transform,

$$DoS(\omega) = \frac{1}{2\pi}\int_{-\infty}^{\infty} e^{-i\omega t}\,\langle v_i(t)\cdot v_i(0)\rangle\, dt.$$

Since Raman and optical Kerr effect (OKE) spectra are modulated by the fluctuation of the polarizability, the $DoS(\omega)$ is often used for qualitative comparison with low frequency Raman data and, in fact, the calculated $DoS(\omega)$ present similar band shapes of OKE and Raman frequency spectra. The low frequency spectra of ILs computed here are roughly comprised of two large overlapped bands centered about ~45 cm^{-1} and ~100 cm^{-1}, corresponding roughly to cations and anions, respectively. For the [emIm]PF_6 system, the $DoS(\omega)$ (Figure 13) indicates the vibrational spectra for the anions span frequencies up to 200 cm^{-1}, whereas the spectra for the cations' is mainly peaked below 100 cm^{-1}.

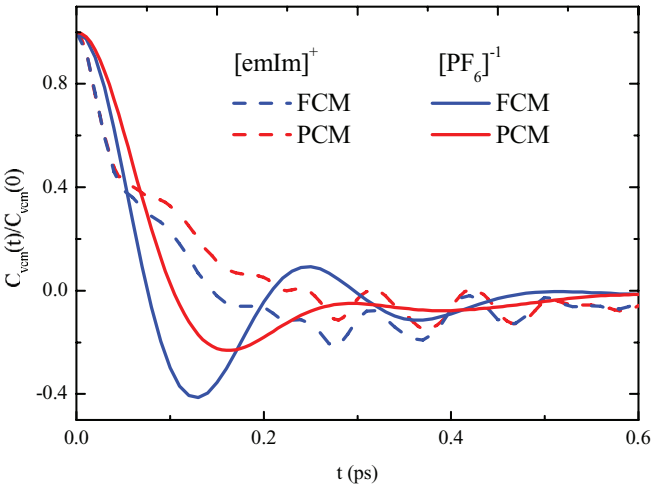

FIG. 12. Single particle time self-correlation functions of the mass velocities, $C_v(t)$, at [emIm]PF_6—at 400 K for the cations (dashed lines) and anions (bold lines) in the polarizable (red lines) and fixed charge model (blue lines).

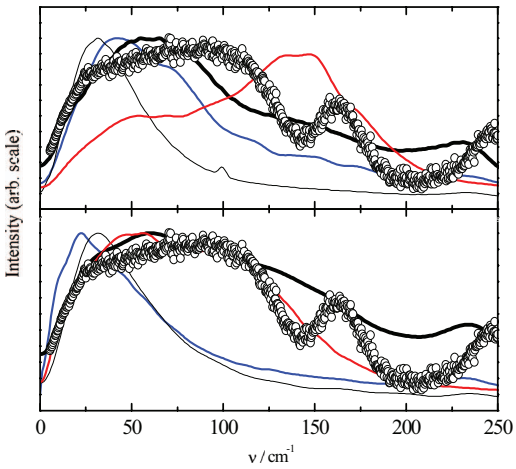

FIG. 13. Vibrational density of states, DoS(ω), calculated for the anions (red lines) e cations (blue lines) for the [emIm]PF_6 using charge fixed (top) and polarizable model. The cations projected DoS(ω) around the NN (black thin lines) and $NN^{\perp}$ (black thick lines) are also shown. The open circles correspond to the low-frequency reduced Raman spectra of the [bmIm]BF_4.

Using fixed charges, the spectra exhibit higher frequency modes for both ionic species. The most pronounced effect of the polarizability is to reduce the relative intensity of the anionic band at ~150 cm^{-1} and enhance the peak at ~50 cm^{-1} (Figure 13, red lines). Interestingly, a similar effect is observed for the density of states computed for the motions of the vector normal to the cationic rings (Figure 13, solid black lines). The experimental Raman spectrum for [bmIm]BF_4,[54] depicted as empty circles in Figure 13, is also shown for comparison. The $DoS(\omega)$ calculated using the polarizable model shows a better agreement with the experimental band shape. Neither models, however, reproduce the experimental spectrum for frequencies above ~150 cm^{-1}.

VI. CONCLUDING REMARKS

In this work, the cations polarizability effects on the equilibrium structural and dynamical properties of some archetypical ionic liquids were evaluated by united atoms MD simulation at a single temperature. For this purpose, using quantum chemistry calculations, a new set of electronegativity equalization method parameters is proposed and its values are correlated to the chemical characteristics of a small family of cations 1-alkyl-3-methyl-imidazolium.

The general characteristics commonly attributed to the ILs are kept with the inclusion of the cationic polarizability, i.e., the charge alternation in the bulk liquid, as depicted by the RDFs, and the greater MSD of the imidazolium cations, despite the larger masses. The structural modifications observed in the ILs systems simulated with polarizable system in comparison to the charge fixed one are: (i) a closer approach of the counter ions in the polarizable model and (ii) a partial transference of the anions preferential positions to places right above and below the center of the imidazolium ring. These features are in agreement with the experimental data on the neutron scattering and are assigned respectively

to the smoothing of the Coulombic interactions and a better distribution of the charges around the imidazolium ring.

Beyond the commonly expected faster dynamics observed in the system simulated with polarizable model, it is worth mentioning that the self-diffusion coefficients obey the natural trend, i.e., the ILs with lower melting points, formed by the PF_6^-, have a greater self-diffusion coefficients than the Cl^- ones as expected since the last have a much greater melting points. The mean residence times makes a clear distinction of the tightly bound anions to the C2 atom and the diffusive crowded population right above and below the center imidazolium ring. As an indication of the importance of polarizability effects for the ILs dynamics, a comparison between the calculated vibrational density of states and the experimental reduced low frequency Raman spectra of the $[bmIm]BF_4$ shows that the agreement is somewhat improved in the polarizable model, although further refinements in the model are clearly necessary.

ACKNOWLEDGMENTS

The authors are indebted to the Brazilian agencies CAPES and FAPESP for the financial support.

[1]M. Revere and M. P. Tosi, Rep. Prog. Phys. **49**, 1001 (1986).
[2]R. D. Rogers and K. R. Seddon, Science **302**, 792 (2003).
[3]P. Walden, Bull. Acad. Imp. Sci. St. Petersburg **8**, 405 (1914).
[4]S. Gabriel and J. Weiner, Ber Dtsch. Chem. Ges. **21**, 2669 (1888).
[5]K. R. Seddon, J. Chem. Technol. Biotechnol. **68**, 351 (1997).
[6]A. Fernández, J. Torrecilla, J. García, and F. Rodríguez, J. Chem. Eng. Data **52**, 1979 (2007).
[7]S. D. Jones and G. E. Blomgren, J. Electrochem. Soc. **136**, 424 (1989).
[8]Z. Hu and C. J. Margulis, Acc. Chem. Res. **40**, 1097 (2007).
[9]D. Camper, J. E. Bara, D. L. Gin, and R. D. Noble, Ind. Eng. Chem. Res. **47**, 8496 (2008).
[10]E. J. Maginn, J. Phys.: Condens. Matter **21**, 373101 (2009).
[11]K. Fumino, V. Fossog, K. Wittler, R. Hempelmann, and R. Ludwig, Angew. Chem. Int. Ed. **52**, 2368 (2013).
[12]S. Tsuzuki, W. Shinoda, H. Saito, M. Mikami, H. Tokuda, and M. Watanabe, J. Phys. Chem. B **113**, 10641 (2009).
[13]*Molten Salts: From Fundamentals to Applications*, NATO Science Series Vol. 52, edited by M. Gaune-Escard (Kluwer Academic Publishers, Dordrecht, 2002).
[14]K. Fumino, A. Wulf, and R. Ludwig, Angew. Chem. Int. Ed. **47**, 8731 (2008).
[15]C. Schröder, Phys. Chem. Chem. Phys. **14**, 3089 (2012).
[16]T. Yan, Y. Wang, and C. Knox, J. Phys. Chem. B **114**, 6886 (2010); **114**, 6905 (2010).
[17]E. I. Izgorodina, Phys. Chem. Chem. Phys. **13**, 4189 (2011).
[18]M. Salanne and P. A. Madden, Molec. Phys. **109**, 2299 (2011).
[19]C. Schröder and O. Steinhauser, J. Chem. Phys. **133**, 154511 (2010).
[20]A. Bagnoa, F. D'Amico, and G. Saielli, J. Mol. Liq. **131–132**, 17 (2007).
[21]C. Schröder, C. Wakai, H. Weingärtner, and O. Steinhauser, J. Chem. Phys. **126**, 084511 (2007).
[22]T. Yan, C. J. Burnham, M. G. Del Pópolo, and G. A. Voth, J. Phys. Chem. B **108**, 11877 (2004).
[23]T. G. A. Youngs and C. Hardacre, Chem. Phys. Chem. **9**, 1548 (2008).
[24]S. Urahata and M. C. C. Ribeiro, J. Chem. Phys. **120**, 1855 (2004).
[25]W. L. Jorgensen, J. D. Madura, and C. J. Swenson, J. Am. Chem. Soc. **106**, 6638 (1984).
[26]H. J. C. Berendsen, J. R. Grigera, and T. P. Straatsma, J. Phys. Chem. **91**, 6269 (1987).
[27]R. T. Sanderson, Science **114**, 670 (1951).
[28]W. Kohn and L. Sham, Phys. Rev. **140**, A1133 (1965).
[29]R. G. Parr and R. G. Pearson, J. Am. Chem. Soc. **105**, 7512 (1983).
[30]T. Taylor, M. Schmollngruber, C. Schröder, and O. Steinhauser, J. Chem. Phys. **138**, 204119 (2013).
[31]P. Bultinck, W. Langenaeker, P. Lahorte, F. De Proft, P. Geerlings, M. Waroquier, and J. P. Tollenaere, J. Phys. Chem. A **106**, 7887 (2002).
[32]Y. Ouyang, F. Ye, and Y. Liang, Phys. Chem. Chem. Phys. **11**, 6082 (2009).
[33]S. L. Njo, J. F. Fan, and B. Van de Graaf, J. Mol. Catal. A: Chem. **134**, 79 (1998).
[34]M. J. Frish, G. W. Trucks, H. B. Schlegel *et al.*, GAUSSIAN 98, Revision A.9, Gaussian, Inc., Pittsburgh, PA, 1998.
[35]W. H. Press, S. A. Teukolsky, W. T. Vetterling, and B. P. Flannery, *Numerical Recipes in Fortran 77: The Art of Scientific Computing*, 2nd ed. (Cambridge University Press, New York, 1992).
[36]J. Dupont and P. A. Z. Suarez, Phys. Chem. Chem. Phys. **8**, 2441 (2006).
[37]O. Borodin, J. Phys. Chem. B **113**, 11463 (2009).
[38]C. Hardacre, S. E. Jane McMath, M. Nieuwenhuyzen, D. T. Bowron, and A. K. Soper, J. Phys.: Condens. Matter **15**, S159 (2003).
[39]M. G. Del Pópolo, R. M. Lynden-Bell, and J. Kohanoff, J. Phys. Chem. B **109**, 5895 (2005).
[40]R. M. Lynden-Bell and T. G. A. Youngs, J. Phys.: Condens. Matter **21**, 424120 (2009).
[41]M. Kanakubo, T. Ikeda, T. Aizawa, H. Nanjo, Y. Kameda, Y. Amo, and T. Usuki, Anal. Sci. **24**, 1373 (2008).
[42]E. I. Izgorodina and D. R. MacFarlane, J. Phys. Chem. B **115**, 14659 (2011).
[43]C. G. Hanke, S. L. Price, and R. M. Lynden-Bell, Mol. Phys. **99**, 801 (2001).
[44]A. Downard, M. J. Earle, C. Hardacre, S. E. J. McMath, M. Nieuwenhuyzen, and S. J. Teat, Chem. Mater. **16**, 43 (2004).
[45]C. Hardacre, J. D. Holbrey, S. E. Jane McMath, D. T. Bowron, and A. K. Soper, J. Chem. Phys. **118**, 273 (2003).
[46]M. Kick, P. Keil, and A. Konig, Fluid Phase Equilib. **338**, 172 (2013).
[47]B. L. Bhargava, S. Balasubramanian, Chem. Phys. Lett. **417**, 486 (2006).
[48]A. Bagno, F. D'Amico, and G. Saielli, ChemPhysChem **8**, 873 (2007).
[49]M. H. Kowsari, S. Alavi, M. Ashrafizaadeh, and B. Najafi, J. Chem. Phys. **129**, 224508 (2008).
[50]S. Urahata and M. C. C. Ribeiro, J. Chem. Phys. **122**, 024511 (2005).
[51]Chem. Phys. Chem. (Special Issue: Ionic Liquids) **13**, 1601 (2012).
[52]C. Schröder, J. Chem. Phys. **135**, 024502 (2011).
[53]H. Tokuda, K. Hayamizu, M. A. B. H. Susan, and M. Watanabe, J. Phys. Chem. B **108**, 16593 (2004).
[54]A. O. Cavalcante, "Low frequency Raman spectra of ionic liquids" (unpublished).
[55]K. A. van Genechten, W. J. Mortier, and P. Geerlings, J. Chem. Phys. **86**, 5063 (1987).